ACOUSTICS 2012

Acoustical monitoring of water infrastructure

K. V. Horoshenkov

University of Bradford, Great Horton Road, BD7 1DP Bradford, UK
k.horoshenkov@brad.ac.uk

Accurate data on the boundary conditions and hydraulic flows in urban water infrastructure, rivers and canals are required to predict accurately the probability of flooding, structural damage, ground subsidence incidents and to optimise the rehabilitation work. Airborne acoustic waves can provide reliable means to measure remotely the hydraulic, operational and structural characteristics of this infrastructure. This talk describes a new acoustical technology developed at the University of Bradford which can be used to detect and locate damage, blockages, sediment deposition, water level variations and hydraulic energy losses in underground networks of pipes. It explains how various pattern recognition methods can be applied to discriminate between the acoustic signatures recorded for a range of conditions and to detect a change. The talk also presents some field work results which prove that the proposed acoustical technology allows for a very rapid, remote inspection of urban water infrastructure which can partly replace more conventional and slower CCTV inspection.

1 Introduction

Acoustic methods for the inspection of pipes to locate blockages and damage have been used extensively with primary applications related to the quality control of pipes. This technology is adopted in petro-chemical engineering, by the oil and gas, and water industries, and in the manufacturing of musical instruments (e.g. [1,2]). Unlike many other inspection methods such as the CCTV, acoustic methods can be fast and non-invasive.

The measurement technique we present in this paper is based on the analysis of acoustic signals that are reflected by various types of irregularities typically found in a pipe which is either dry or only partially filled with water. These reflections carry sufficient information to identify structural defects, sediment blockages, lateral connections, pipe ends and the level of water which this pipe carries. Traditionally, sound pressure data are used to carry out the feature extraction and classification analysis (e.g. [1,2]). The technology which we present here makes use of acoustic intensity data. Unlike acoustic pressure, acoustic intensity is a vector which direction is perpendicular to the wave front, i.e. the direction in which the acoustic energy propagates. This quantity is very sensitive to the changes in the medium properties and to the changes in the boundary conditions along the path of the sound wave. Sudden changes in the medium properties result in acoustic reflection and scattering. A main advantage in the acoustic intensity approach is that it can be used to separate waves reflected in a particular direction. These data can be used more robustly in a suitable condition classification model than the acoustic pressure data.

The purpose of this paper is to explain the basic technology which has been developed at the University of Bradford to detect changes in a pipe carrying a flow of water and to illustrate a range of conditions which affect propagation of acoustic waves in a pipe. This technology combines the acoustic instrumentation, signal processing algorithms and pattern recognition methods.

2 The acoustic theory

There are a number of problems in using acoustic waves for the detection of the conditions in live underground pipes. Although the technology for the pipe bore reconstruction has been developed a while ago (e.g. ref. [2]), it is impractical to use it in a relatively large diameter partially-filled underground pipes which cannot be terminated from one end. The only practical way to survey this type of pipes is to insert an acoustic sensor through an inspection manhole and secure it just above the flow of water as shown in Figure 1. Since it is common to inspect pipes in the dry flow conditions, i.e. when the level of water is relatively low, a large proportion of the pipe circumference is relatively dry and it can be inspected with airborne acoustic waves. Because of the huge mismatch between the impedance of air and that of the pipe wall material, the coupling between the airborne waves and structure-borne waves in the pipe wall is very small and can be neglected in the model. In this way, the acoustic wave reflections which occur due to the cross-sectional changes and wall impedance variation can be timed in terms of the airborne wave velocity, which is a relatively unsophisticated process.

A main problem here is that the sensor cannot be inserted far enough into the pipe so that the reflected waves arrive on to the sensor microphones from a plurality of directions as shown in Figure 1. These reflections cannot be separated if only one sensor microphone is used. An alternative here is to use a directional array of microphones. However, this is impractical to implement in a pipe as the length of such an array is required to be much longer than the wavelength. This instrument will be long and difficult to deploy and maneuver in the manhole and pipe environment.

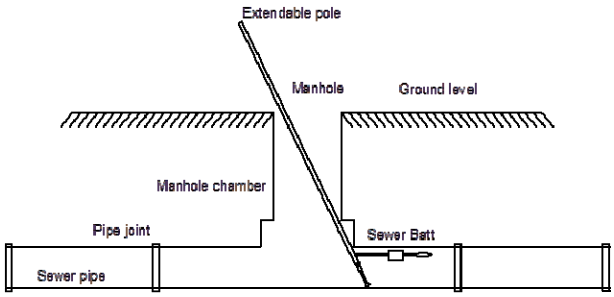

Figure 1: The principle of the acoustic sensor deployment in a life underground pipe.

One simple solution to this problem is to use the acoustic intensity probe. In this probe signals from two or more closely spaced microphones can be combined and used to determine the amplitude of the reflected waves and the direction from which these waves have arrived. Therefore, a key element of this technology is the calculation of the instantaneous acoustic intensity vector, which is carried out by combining the acoustic pressure signals from an array of closely spaced microphones. The instantaneous intensity vector is given by the following expression

$$\tilde{\boldsymbol{I}}(t) = p(t)\boldsymbol{u}(t), \quad \boldsymbol{u}(t) = -\frac{1}{\rho_0}\int_{-\infty}^{t}\frac{\partial p}{\partial \boldsymbol{n}}d\tau, \qquad (1)$$

where $\mathbf{u}(t)$ is the time-dependent acoustic (particle) velocity vector, $\mathbf{n}$ the normal that coincides with the direction of sound propagation and $p(t)$ is the acoustic pressure

measured at the receiver position. The main difficulty here is to determine the exact value of the $\frac{\partial p}{\partial \mathbf{n}}$ quantity and its approximate value is commonly used so that equations (1) are rewritten as

$$p(t) \approx \frac{p_m(t) + p_n(t)}{2}, \quad \mathbf{u}(t) \approx \frac{1}{\Delta \rho_0 \mathbf{n}} \int_{-\infty}^{t} \left[p_m(\tau) - p_n(\tau) \right] d\tau, \tag{2}$$

where $p_m(t)$ and $p_m(t)$ are the sound pressures measured on two microphones in the array that are separated by the distance $\Delta << \lambda$, λ being the acoustic wavelength.

Sound propagation in a cylindrical pipe above the frequency of the 1st cross-sectional mode is a dispersive phenomenon. In this frequency range sound waves can propagate in directions other than normal with respect to the cross-section of the pipe, and the sound pressure depends strongly on the source and receiver positioning. Therefore, it makes sense to study the behaviour of the sound intensity in the plane wave regime i.e. in the frequency range below the 1st cut-on frequency of the pipe. In this way, the sound pressures recorded with the microphone array can be conditioned and filtered in several narrow frequency bands using a suitable digital filter. The intensity response between microphone *m* and microphone *n* in the microphone array can then be determined for each individual frequency band according to expression (2). The result can be divided by the norm, i.e.

$$\left\| I_{mn} \right\| = I_{mn} \left| \max_{t \le T_0} \left[-I_{mn}(t) \right] \right|^{-1} \tag{3}$$

where T_0 being some time limit which relates to the duration of the incident pulse. This normalisation procedure ensures that the maximum intensity in the incident sound wave is equal to or less than -1. In the case, when the microphone array is linear and it is orientated in the direction of plane wave propagation, the normalised intensity response for individual microphone pairs can be compensated for the time shift, τ_{mn}. This time shift is present in the intensity response because of the variable distance from the speaker diaphragm to the centre of a microphone pair in the array, i.e.

$$e_{mn}(t) = I_{mn}(t + \tau_{mn}) / \left\| I_{mn} \right\|. \tag{4}$$

The normalized and time-shift compensated intensity responses for several microphone pairs can then be combined coherently to obtain the mean intensity response function

$$e(t) = \sum_{m,n} e_{mn}(t) \ . \tag{5}$$

In this way the effects of sound reflection from the pipe termination near the acoustic instrument and mismatch errors are reduced. Only the positive (reflected) part of the mean intensity response function (5) is needed for the pipe condition characterization which represents the sound intensity reflected from the irregularities in the pipe, i.e.

$$e^{+}(t) = \left(e(t) + \left| e(t) \right| \right) / 2 . \tag{6}$$

3 The instrument

The instrument which was developed at Bradford to implement the acoustic technology detailed in section 2, consists of an acoustic sensor which comprises a microphone array and a speaker. The instrument also includes a data acquisition module, ruggedized laptop and cables (see Figure 2). The spacing between the microphones in the microphone array is chosen to be considerably less than the wavelength to allow for the intensity measurements. The microphones can be spaced non-equidistantly to optimize the accuracy of the intensity measurements in a broad frequency range. An array of non-equidistantly spaced microphones enables to obtain a maximum number of microphone pairs separated by unrepeated distances. A water resistant speaker which is capable of reproducing a broad frequency range is used as a source of sound. Signal generation for excitation, acquisition and processing are controlled with the PC via an electronic microcontroller which is connected with a USB cable (see Figure 2).

Figure 2: Instrument prototype equipment.

A sine chirp is used as an excitation signal. This signal is time-invariant and it is less prone to harmonic distortions. This kind of stimulus is well suited for measurements in the presence of a dynamically rough water surface and high levels of background noise. Once received on a microphone, this signal is deconvolved to obtain an acoustic pressure impulse response using the procedure detailed in ref. [3]. It can be filtered and used in the intensity analysis detailed in the previous section. An example of the resultant acoustic intensity response calculated for a clean 150mm pipe (eq. (6)) is shown in Figure 3. A reflection from the pipe end is visible clearly in the intensity response at 14.8m.

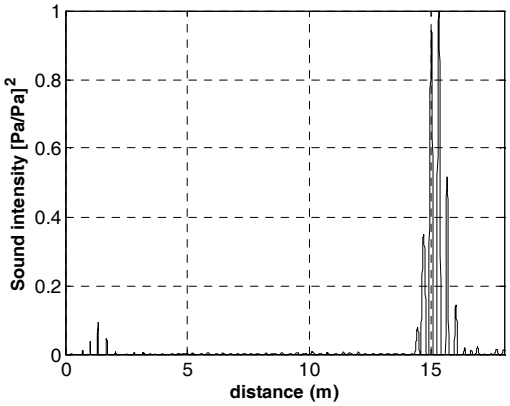

Figure 3: The positive intensity response for a clean, 14.8m long pipe with 150mm diameter (150-300 Hz range).

4 Pattern recognition and classification

It is impractical to apply the bore reconstruction methods (e.g. [1,2]) in a partly-filled pipe buried beneath the ground. A main problem here is a lack of good quality reference pulse which is required for the layer peeling method with which the exact pipe cross-section can be reconstructed as a function of distance. However, it is practical to collect a number of acoustic signatures which can be then used to construct a signature library (a database) which can then be adopted in a correlation analysis or used with a suitable statistical method to recognise with a good degree of probability a particular condition which is typically for a buried, partly-filled pipe.

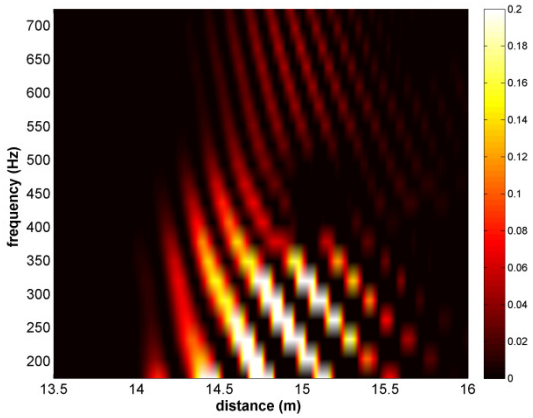

Figure 4: The acoustic signature of a typical pipe end presented in the form of a spectrogram.

An example of an acoustic signature is shown in Figure 4 which presents the spectrogram of the acoustic reflection from the end of a clay pipe. The temporal and spectral characteristics of this reflection are unique to the end of a 150mm pipe and these can be exploited to recognise the pipe conditions from the recorded acoustic intensity response in way similar to that automatic voice recognition is carried out. Two particular algorithms can be used for this purpose: direct cross-correlation in the time and frequency domains and hidden Markov models.

The cross-correlation algorithm proposed here involves finding the normalized 2-D correlation function

$$r(t,\omega)=\frac{\int_0^{\omega_{\max}}\int_0^{T_{\max}} e^{+}(\tau,\varpi)e_s^{+}(t-\tau,\omega-\varpi)d\tau d\varpi}{\int_0^{\omega_{\max}}\int_0^{T_{\max}} e^{+}(\tau,\varpi)e^{+}(t-\tau,\omega-\varpi)d\tau d\varpi \int_0^{\omega_{\max}}\int_0^{T_{\max}} e_s^{+}(\tau,\varpi)e_s^{+}(t-\tau,\omega-\varpi)d\tau d\varpi} \quad (7)$$

where $e^{+}(t,\omega)$ is the frequency-dependent mean intensity response function calculated from the measured data and $e_s^{+}(t,\omega)$ is a mean intensity response function representing a defect signature selected from the library (signature database). The bounds in the integrals in expression (7) are selected to ensure that the correlation analysis is carried out over a representative temporal period, $T_{\max}$, and range of frequencies, $\omega_{\max}$, which are sufficient to capture the key features of a particular condition in the sewer pipe. In the above analysis a threshold of $r(t,\omega)$ can be set to trigger a match between the recorded data and a signature stored in the signature database.

Alternatively, the signature of an irregularity in a pipe can be used as the physical process which can be described probabilistically with a hidden Markov model (HMM)[4]. The statistical properties of the reflected sound wave undergo a series of transitions and different spectral patterns can associate with different type of irregularity and other conditions present in the pipe at the time of measurement. These spectral and temporal patterns can be characterized by distinctly different statistical properties, which are in turn reflected in transitions of the defect signal from one statistical state to another.

In order to create a HMM, one needs to guess the number of sources that emits observation and the number of states with which these sources can be associated. Each state is an emitting source statistically described by the respective probability density function. Therefore, the probability density describing each of these states is $b(k\,|\,i)=P(y_t=k\,|\,x_t=i)$ where i =1,2,..,S, S is the number of states, x_t is the state random process, $1\le k\le K$, K is the number of distinct observation symbols per state, y_t is the observation random process. Since the process undergoes random jumps from one state to another, the model should also have access to the set of state transition probabilities, $a(i\,|\,j)=P(x_t=i\,|\,x_{t-1}=j)$ where i, j =1,2,..,S, and $P(i\,|\,j)$ is the probability of the system jumping from state j to state i. Finally, since any observation sequence must have an origin, it is necessary to know the probability of the first observation being emitted by state i. The K-by-S observation probability matrix, B, the S-by-S state transition matrix, A, and the initial probability matrix, π, are then given by

$$B=\begin{pmatrix} P(1\,|\,1) & \cdots & P(1\,|\,S) \\ \vdots & \ddots & \vdots \\ P(K\,|\,1) & \cdots & P(K\,|\,S) \end{pmatrix},\quad A=\begin{pmatrix} P(1\,|\,1) & \cdots & P(S\,|\,1) \\ \vdots & \ddots & \vdots \\ P(1\,|\,S) & \cdots & P(S\,|\,S) \end{pmatrix},\quad \pi=\begin{pmatrix} P(1) \\ \cdots \\ P(S) \end{pmatrix} \quad (8)$$

In this case, we can design a HMM, $\lambda=(B,A,\pi)$, and examine whether the probability (likelihood) $P(y\,|\,\lambda)$ is sufficiently high for this model to represent the observation sequence, $y=\{y_1,y_2,...,y_T\}$. In a simple word, we assume that one of the existing hidden Markov models which we build would be able to reproduce the pattern in the data recorded in the field. In the case of sound propagation in a pipe with a defect, the acoustical signature of this defect is associated with the HMM via the highest likelihood for which the defect can be recognized.

5 Detection of change

In practical applications to underground pipe management it is often desirable to determine the degree of change which a section of a pipe has experienced over time. Such operational and structural changes are often not localised and occur gradually along the whole length of the pipe resulting from the development of longitudinal cracks and continuous sedimentation. At some critical instant a small change can result in a service failure (which may then contribute to a flood event caused by a blockage or a structural pipe collapse). A small change in pipe conditions

is notoriously hard to detect directly, particularly when the pipe consists of several, poorly joined sections. Thus, the pipe is not simple or 'ideal'. If the acoustic measurement is taken from an open end of the pipe connected to an inspection cavity of complex geometry, then it can be extremely difficult to separate the effects of the cavity from that of the pipe via the acoustic response. Thus, the impedance conditions can be difficult to model.

An alternative method here is to use the so-called matched field processing (MFP)[5] which is able to detect changes in a continuous or non-continuous air-filled pipe. The MFP concept is relatively simple. We record the acoustic response of a pipe, $f_m(t)$ using $m = 1,..., N$ number of microphones and calculate its short-time Fourier transform

$$F_m(\omega, t_0) = \int_{t_0}^{t_0+K\Delta t} f_m(t) e^{-i\omega t} dt,$$

where t_0 is an instant on a sliding time scale. If the pipe changed, then its acoustic response should also change. The new acoustic response, $g_m(t)$, which we will record, should be dissimilar to $f_m(t)$. The degree of similarity between these two states can be estimated using the ambiguity surface function which is given by the following expression

$$\mathrm{AMS}(\omega, t_0) = \frac{\left|\sum_{m,n} F_m^* F_n G_m G_n^*\right|}{\left|\sum_m F_m^* F_m\right| \left|\sum_m G_m^* G_m\right|}, \qquad (9)$$

where

$G_m(\omega, t_0) = \int_{t_0}^{t_0+K\Delta t} g_m(t) e^{-i\omega t} dt$ and * denotes the complex conjugate. It is easy to illustrate that this function is bounded $0 \le \mathrm{AMS}(\omega, t_0) \le 1$, and that $\mathrm{AMS}(\omega, t_0) = 1$ corresponds to the perfect match. The above analysis can be applied either to the acoustic pressure or instantaneous intensity data. The only requirement here is that the number of microphones (receivers) should be $N \ge 2$.

6 Estimation of the water level

The acoustic impulse response recorded in a pipe can also be used to determine the level of water or wet sediment above which the sensor is installed. The level of water or wet sediment affects the frequencies of cross-sectional modes that can propagate in the pipe. At these frequencies the modal phase velocity is close to the infinity and the acoustic field in the pipe has characteristic maxima that can be detected with a narrow-band frequency analysis. In this way the resonance peaks in the frequency spectra in the recorded acoustic impulse response can be related to the water/sediment level. Figure 5 presents the dependence of the frequency of the first cross-sectional mode in a 150mm pipe on the level of water. Clearly, the modal frequency increases with the increased level of water. This results is measured in the laboratory and predicted using a finite element model in which the boundary admittance was assumed $\beta = 0$. This dependence can be expressed with the following simple expression

$$w_a = 0.05874 f_w - 80.11, R^2 = 0.994, \qquad (9)$$

which is likely to scale for pipes which diameter is not equal to 150mm because the frequency of the 1st cross-sectional mode $f_w = 0.59c/d$ when $w_a = 0$. Here c is the speed of sound in air and d is the pipe diameter.

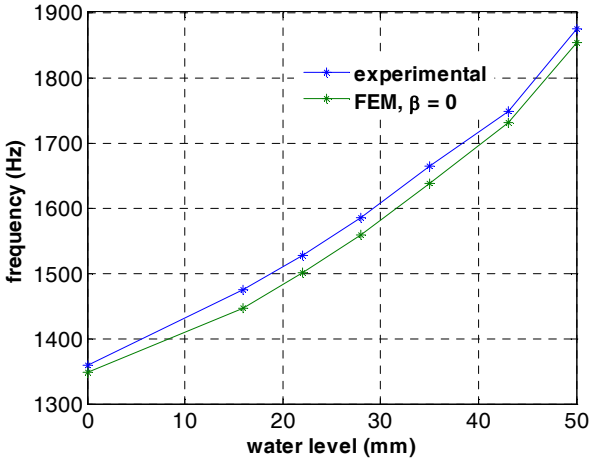

Figure 5: The measured and predicted relations between the frequency of cross-sectional modes and the level of water in a 150mm pipe.

7 Estimation of sediment level

A common problem for underground pipes is the development of a sediment layer at the pipe bottom, wall corrosion, erosion or incrustation. The effect of these changes on the acoustic wave propagation is somewhat similar: an apparent increase in the attenuation and a shift in the frequency of cross-sectional modes which can be excited in the pipe. The solution of this problem is to combine a finite element and normal mode decomposition techniques to calculate the acoustic pressure field, *p*. The acoustic pressure in the pipe can be determined from following matrix equation

$$[K]p + jk[D]p + k^2[M]p = 0, \quad (10)$$

where k is the wavenumber and $[K] = -\iint_S \nabla N_i \bullet \nabla N_j dxdy$, $[D] = \oint_l N_i N_j \beta_{ij} dl$, $[M] = \iint_S N_i N_j dxdy$, are the stiffness, damping and mass matrices, respectively $(i, j = 1,2,....V)$. In the above expressions N_i are the interpolated shape functions in the finite element formulation, β_{ij} are the values of the normalised surface admittance, *S* is the cross-sectional area and *l* is the circumference of the duct.

The inverse admittance problem is defined such that if the modal frequencies and their corresponding attenuations are given, then the surface admittance of the absorbing lining needs to be reconstructed. We assume that the geometry of the duct and the properties of the fluid content

(e.g. air) are known, i.e. the matrices $[K]$ and $[M]$ are predetermined and complete. We use the optimisation principle and equation (10) to minimise the following objective function $f(\mathbf{x})$

$$\min\left(f(\mathbf{x}) = abs\left\{\det([K]+ik[D]+k^2[M])\right\}\right), \qquad [D]\in R^N \tag{11}$$

where $[D]$ is the unknown damping matrix that contains the complex values of the surface admittance associated with the existence of the porous sediment or wall imperfections. Here $\mathbf{x}$ is the parametric vector related to the unknown value of the complex surface admittance and the wavenumber k is associated with the modal frequency and its attenuation. It is expressed by

$$k = f_{mn}\times 2\pi/c + \alpha_{mn}\times i/8.685, \tag{12}$$

where f_{mn} and α_{mn} are the modal frequency and attenuation, respectively. If the acoustic lining is uniform, then only one frequency-dependent surface admittance for the boundary needs to be calculated. In this case $N = 2$ and there are two sets of variables in equation (10): one is for the real part and another is for the imaginary part of the admittance. The problem becomes much more complicated if more elements with different values of the surface admittance $\beta_{ij} \neq \beta_{vw}$, $i \neq v, j \neq w$ are introduced as new unknowns. A simple wave to solve optimisation problem (11) is to use the direct search method[6].

Figure 6: The method for sensor deployment in a live (300mm) sewer in the field.

The above method was applied to invert the parameters of a 70mm thick layer of marble stone which was laid on the bottom of a 20m long, 600mm diameter concrete pipe as shown in Figure 6[7]. The relative sound pressure level was acquired as a function of time. The acoustic pressures were recorded on an array of microphones, filtered using a 6-th order Butterworth digital pass-band filter that was tuned to the frequencies of the first three cross-sectional modes. The width of the spectral window was set to 330 – 370 Hz for mode (1-0), 540-620 Hz for mode (2-0), 680-730 Hz for mode (0-1). The comparative data were: (i) the admittances measured by the standard impedance tube method; (ii) admittances predicted by the acoustic impedance model[8]. The higher-order modes were neglected because of the ambiguity caused by stronger modal coupling due to sediment roughness and progressively non-locally reacting behaviour of the sediment. The results of this analysis are summarised in Table 1, which presents the inverted real and imaginary parts of the surface admittance and the surface admittance data determined with the direct means.

Table 1: Comparison of the acoustic admittances obtained by the three methods for the 70mm thick layer of marble stone in the 600mm pipe.

Mode	Admittance by inverse method	Admittance by tube measurement	Admittance by Voronina model[8]
(1-0) (360Hz)	0.012+0.156i	0.0136+0.177i	0.0130+0.162i
(2-0) (600Hz)	0.037+0.236i	0.040+0.256i	0.035+0.225i
(0-1) (714Hz)	0.0453+0.13i	0.056+0.285i	0.051+0.210i

The results shown in Table 1 suggest that the inversed values of the acoustic surface admittance agree well in general with those measured or predicted directly. Specifically, the maximum relative error in the inversed real and imaginary parts of the acoustic surface admittance is limited to 11% in the case of the (1-0) and (2-0) modes. In the case of the (0-1) mode, the relative error in the real and imaginary part of the admittance is 19% and 54%, respectively. The loss of accuracy is mainly attributed to the effect of sediment roughness which can be accounted for if the mean roughness height, ε, is included in the expression of the admittance as suggested by Attenborough [9]

$$\beta_{rough} = -ik_0\varepsilon + \beta_{smooth}, \tag{13}$$

where β_{smooth} is the surface admittance of a perfectly smooth sediment layer, and k_0 is the wavenumber in air. This relation suggests that the mean roughness height of the marble stone layer in the 600mm concrete pipe is required to be 12mm in order to compensate for the 54% discrepancy between the inversed and directly measured values of the imaginary part of the acoustic surface admittance. This compensation is acceptable considering the characteristic dimension of the marble stones in the sediment is 7.3mm.

8 Condition detection and classification

The acoustic pipe inspection system presented in the previous sections has been tested in the laboratory and in the field. In the laboratory the system was tested to discriminate between a blockage, lateral connection and the pipe end. It was also tested to detect a change in the pipe and to monitor the evolution of a sediment build-up in the presence of flow. Figure 7 shows the method of sensor deployment in a live sewer in the field. The sensor is

attached to an extendable pole which is lowered in the manhole chamber so that the speaker and the microphone array are positioned above the flow level.

Figure 7: The method for sensor deployment in a live (300mm) sewer in the field.

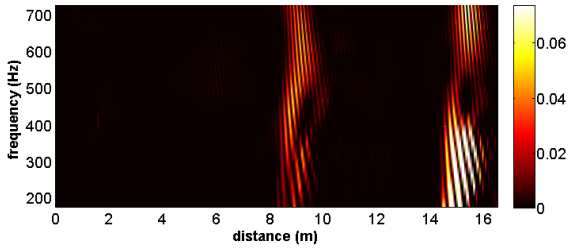

Figure 8: The acoustic intensity spectrogram recorded in a 14.8m clay pipe with a blockage.

Figure 8 shows the spectrogram of the acoustic intensity response obtained in the laboratory for a 14.8m long, 150mm diameter clay pipe with a 25% blockage. The spectrogram shows two clear reflections: at 8m from the sensor and at 14.6m from the sensor. These reflections correspond to the blockage and open end of the pipe, respectively.

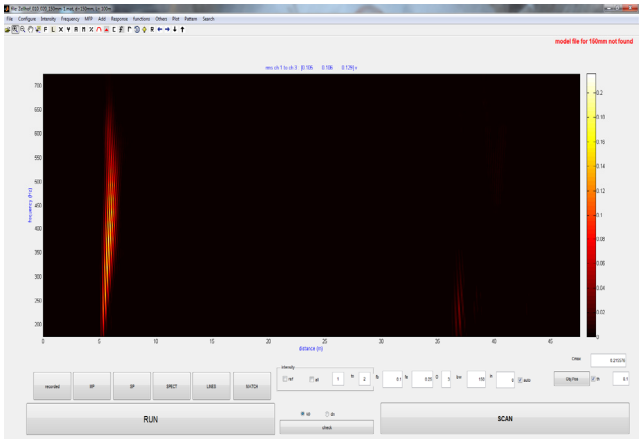

Figure 9: The acoustic intensity spectrogram recorded in a 14.8m clay pipe with a blockage.

Figure 9 presents the view of the software GUI interface which was developed for operating in the field. This interface incorporates all the functions which are discussed in the previous chapters. The spectrogram shown in Figure 9 was recorded in a clean, 150mm diameter live sewer near Salzburg in Austria. The first reflection which occurs at 5m from the sensor end corresponds to a lateral (house) connection. The second reflection which occurs at 37m corresponds to the farther pipe end.

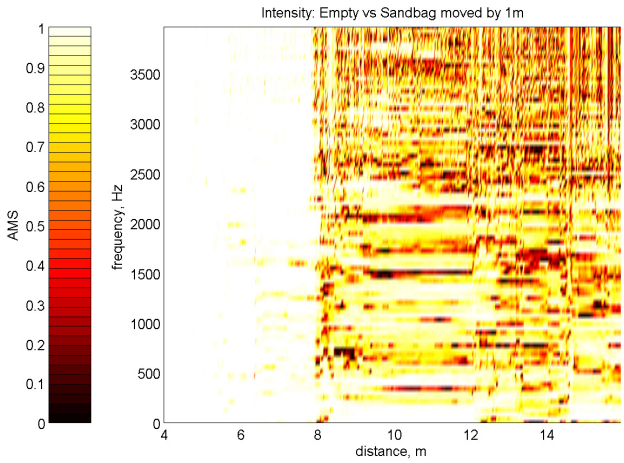

Figure 10: The ambiguity surface calculate for a 14.8m clay pipe with a blockage at 8m.

Figure 10 presents the ambiguity surface for the 150mm clay pipe with a 25% blockage at 8m. The result presented in Figure 10 was obtained by recording the response of a clean pipe and using it as a reference data in eq. (9) against that which was recorded after a bag filled with silt sediment had been deposited in the pipe. The result illustrates clearly the position at which this change in the pipe conditions has developed and the colour intensity illustrates the severity of this change.

Table 2 presents the statistical data on performance of the two cross-correlation pattern recognition and classification methods presented in section 4. This algorithm was applied to the acoustic data collected in the 150mm pipe from 30 independent experiments. The following abbreviations are adopted here: PE – pipe end; BK –blockage; LC – lateral connection. The presented data for $< r >$ correspond to the percentage of correct classifications, which is the ability of the cross-correlation algorithm to match the data with a particular condition in the presence of a variable flow level, variable sensor position and intermediate artefacts introduced into the path of the propagated acoustic wave. ∂r corresponds to the standard deviation in the cross-correlation data taken over the whole range of experiments.

Table 2: Performance of the cross-correlation algorithm.

File group	Cross-correlation of test signatures with the signatures stored in the library (i.e. pipe end , blockage and lateral connection)			
	$< r >$			∂r
	PE	BK	LC	
PE	96.5	71.4	21.4	9.4
BK	80.8	99.2	1.4	1.6
LC	67.9	11.3	88.9	33.3

Table 3 presents the data which illustrate the ability of the hidden Markov model to identify three different conditions in a 150mm clay pipe. The presented numerical values correspond to the logarithmic measure of the likelihood calculated for the guessed condition according to the

method detailed in section 4. The smaller the value of $\log < P(y \mid \lambda) >$, the smaller the likelihood that the data would match that particular condition. The standard deviation in the likelihood, $\partial P(y \mid \lambda)$, corresponds to the variability in $P(y \mid \lambda)$ taken over the range water flow levels, sensor positions and intermediate conditions in the pipe.

Table 3: Performance of the hidden Markov models.

Likelihood of test signatures with three Hidden Markov Models (i.e. pipe end , blockage and lateral connection)				
$\log < P(y \mid \lambda) >$			guess	$\partial P(y \mid \lambda)$
PE	BK	LC		
-18.7	-68.9	-224.7	PE	0.26
-252.0	-22.8	-242.0	BK	2.83
-231.2	-268.8	-22.7	LC	4.36

The same two algorithms have been applied to the data collected in the field around the UK and in Austria in 150mm, 225mm and 300mm diameter pipes. The results of the pattern recognition data analysis were compared against the CCTV reports provided by the water and sewer inspection companies. The results show that the cross-correlation algorithm is able to recognise correctly 67% of the lateral connection and pipe end conditions. The results also show that the hidden Markov model is more robust because it can recognise correctly 94% of these conditions.

9 Estimation of hydraulic roughness

The water industry uses mathematical models for water pipes to predict flow depth, velocity and hydraulic capacity. These models are essential tools in the design process for rehabilitating existing ageing pipes and assessing their propensity for flooding and discharges to watercourses. Bed sediments, pipe obstructions and general pipe roughness can considerably affect the theoretical predictions. A major problem for sewer flow modellers and operators is to define the physical value of the roughness coefficient, k_s, that cannot be measured directly. This value is need to determine the hydraulic energy (head) loss, h_f, from which the water flow level and velocity can be estimated for a given flow discharge. Where sediment deposits exist, they simultaneously constrict the cross section of the sewer, and increase the effective boundary roughness, increasing the water level for a given discharge, increasing the hydraulic head loss and reducing the pipe flow capacity.

Acoustic technology provides the possibility to link the acoustic reflection strength of sediment deposited in a pipe with the hydraulic head losses. If the wetted cross-section of the pipe undergoes a change, then the water flow is likely to be affected and the water surface will no longer appear uniform. In the case when a blockage is deposited at the bottom of a partly-filled pipe, the flow level will inevitably increase in the vicinity of this blockage so that the water can continue flow over the top of this blockage as along as the blockage does not occupy the total cross-section of the pipe. The hydraulic effect of a blockage is shown in Figure 11 which presents the experimental data on the water flow level measured in a 150mm pipe in the presence of blockages with variable height.

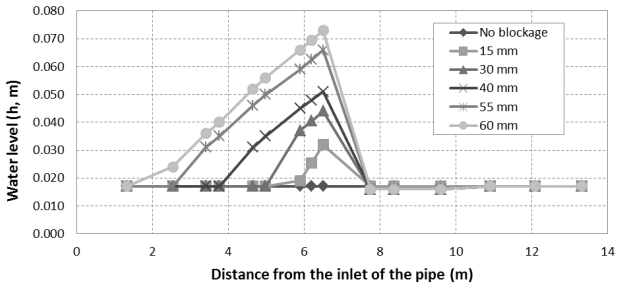

Figure 11: Water depth values for clean and blocked pipe for flow discharge of Q=0.42 litre/s, pipe diameter 150mm.

Clearly, an apparent increase in the water level caused by the presence of the blockage inevitably results in a proportion of the energy in the incident acoustic wave reflected in the direction of the sensor. Here, it is logical to assume that the greater the variation in the water level caused by the presence of a local blockage, the greater the hydraulic head loss and the reflected acoustic energy. In this way, the reflected acoustic energy and the hydraulic head loss can be linked to determine non-invasively the hydraulic roughness of a particular section of the pipe. Figure 12 shows the spectrogram of the acoustic intensity response reflected from a 15mm blockage completely surrounded by a flow of water.

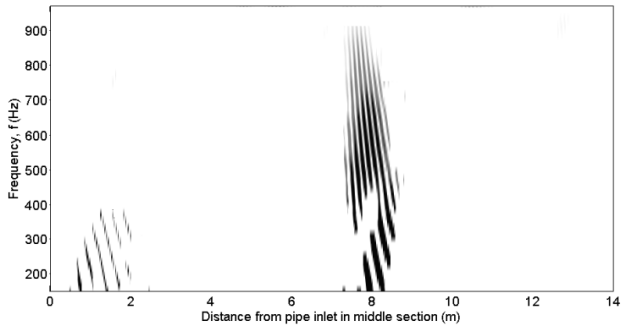

Figure 12: The intensity spectrogram for the 150mm pipe with a 15mm high blockage for 1.00 litre/s discharge.

The intensity shown in Figure 12 can be integrated to determine the reflected acoustic energy, i.e.

$$E_T = \iint_{t,\omega} e^{+}(t,\omega)\, dt\, d\omega . \qquad (14)$$

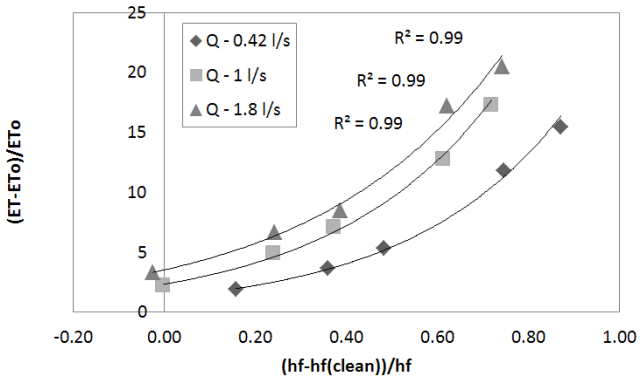

Figure 13: The relation between the energy in the reflected acoustic wave and the hydraulic head loss in the 150mm pipe.

The hydraulic head loss can be estimated from the data shown in Figure 11 using the Darcy- Weisbach equation[10]

$$fV^2 L_{21} = 8gRh_f \qquad (15)$$

where f is the Darcy friction coefficient, L_{21} is the length of the pipe containing the blockage, V is the local mean flow velocity, g is the gravity acceleration and R is the hydraulic radius.

Figure 13 presents the results of this analysis for a range of hydraulic conditions in the 150mm pipe. The results are presented here in terms of the dimensionless quantities $(h_f - h_{f,clean})/h_f$ and $(E_T - E_{T,0})/E_T$, where $h_{f,clean}$ and $E_{T,0}$ are the hydraulic head loss and the reflected acoustic energy measured in the pipe without any blockage, respectively. The data presented in Figure 13 suggest that unambiguous relations exist between the hydraulic head loss and acoustic energy reflected by a local blockage in a partly-filled pipe. The use of such simple sensing technology offers the opportunity to monitor pro-actively developing of blockages and calibrate better the numerical tools for modelling the hydraulic flow.

10 Conclusions

Acoustics provides a very powerful tool for the inspection of hydraulic, structural and operational conditions in pipes and open channels. Acoustic methods are remote and non-invasive. A new technology and instrumentation based on acoustic intensity data has been developed and used to inspect live underground water pipes in the laboratory and in the field. This technology is robust, non-invasive and rapid. It combines acoustics, signal processing and pattern recognition methods. Unlike the CCTV inspection, the speed of the acoustic survey does not depend on the length of the pipe and only limited by the speed with which the acoustic data can be communicated and processed. The currently technology enables the inspection process to be completed within one minute.

It has been shown that the recorded acoustic signals can be processed in a plurality of ways. For this purpose suitable software and GUI interface have been developed to be used on a ruggedised tablet PC. Acoustic data can be easily stored to form a digital database of acoustic signatures. These data, together with the signatures recorded in a database, can then be used to detect changes in a pipe and estimate their severity. The acoustic signals can also be used to locate blockages and structural defects, determine the level of water, amount and nature of deposited porous sediment and to estimate in-situ the hydraulic energy losses in live sewer pipes. The latter cannon be done at present with any other method.

Live pipes are very complicated, dynamic systems which require robust signal processing and pattern recognition methods to measure accurately and understand well the nature of overall change and to discriminate between localised changes. As a result, there are several challenges which are yet to be overcome. Firstly, it is difficult to use low-frequency acoustic waves (i.e. the plane wave regime) to discriminate between multiple defects which are closely spaced in the pipe. Secondly, it is difficult to make use of higher frequencies and higher order modes because of the strong variation in the acoustic pressure with the sensor position beyond the first cross-sectional mode. Thirdly, the presence of porous sediment results in a considerable acoustic attenuation and the pressure in acoustic waves reflected from farthest locations in the pipe can be weakened below the noise threshold. Fourthly, more work is needed to develop acoustic sensors which are extremely robust and completely water-proof.

Acknowledgments

The author would like to acknowledge the contribution to this work from the following research staff and PhD students at Bradford: Dr. Tareq Bin Ali, Dr Chan H. See, Mrs A. Romanova and Mr. Andreys Fedotovs. The equipment used in this work has been, by and large, manufactured by the following technical staff at Bradford: Mr. Antony Daron, Mr. Allan Robinson, Mr. Ken Howell, Mr. Nigel Smith and Mr. D. Chavda. The author would like to thank the industrial collaborators on this project. This work was supported by the UK's Engineering and Physical Sciences Research Council (Grants EP/D058589/1, EP/G005737/1) and by the Brian Mercer Award from the Royal Society of London.

References

[1] M. H. de Salis and D. J. Oldham, "Determination of the blockage area function of a finite duct from a single pressure response measurement," *J. Sound Vib.* 221, 180-186 (1999).

[2] D. B. Sharp and D. M. Campbell, "Leak detection in pipes using acoustic pulse reflectometry," *Acta Acustica united with Acustica*, 83, 560-566 (1997).

[3] M. T. Bin Ali, *Development of Acoustic Sensor and Signal Processing Technique*, PhD Thesis, University of Bradford, Bradford, UK (2010)

[4] L. E. Baum, "An inequality and associated maximization technique in statistical estimation for probabilistic functions of Markov processes," *Inequalities* 3, 1-8 (1972).

[5] A. Tolstoy, *Matched Field Processing for Underwater Acoustics*, World Scientific Publications, Singapore, 1993.

[6] G. R. Reklaitis, A. Ravindran and K. M. Ragsdell, *Engineering Optimization Methods and Applications*, John Wiley and Sons (1983).

[7] Y. A. Yin and K. V. Horoshenkov, "Remote characterization of the acoustic properties of porous sediments in a multi-modal round pipe," CD-ROM *Proc. Inst. Acoust*. 28(1), Southampton (2006).

[8] N. N. Voronina and K. V. Horoshenkov, "A new empirical model for the acoustical properties of loose granular media," *Appl. Acoust*., 64(4), 415-432 (2003).

[9] K. Attenborough and S. Taherzadeh, "Propagation from a point source over a rough, finite impedance boundary," *J. Acoust. Soc. Am*., 98(3), 1717-1722 (1995).

[10] L. F. Moody, "Friction factors for pipe flow," *Trans. ASME*, 66(8), 671-684 (1944).